IOPscience iopscience.iop.org

Home Search Collections Journals About Contact us My IOPscience

Surface resistance and field emission current measurements on chemically vapour deposited polycrystalline diamond measured by scanning probe methods

This article has been downloaded from IOPscience. Please scroll down to see the full text article.

2004 J. Phys.: Condens. Matter 16 S171

(http://iopscience.iop.org/0953-8984/16/2/020)

View the table of contents for this issue, or go to the journal homepage for more

Download details:
IP Address: 129.252.86.83
The article was downloaded on 28/05/2010 at 07:15

Please note that terms and conditions apply.

INSTITUTE OF PHYSICS PUBLISHING JOURNAL OF PHYSICS: CONDENSED MATTER

J. Phys.: Condens. Matter **16** (2004) S171–S179 PII: S0953-8984(04)66981-5

Surface resistance and field emission current measurements on chemically vapour deposited polycrystalline diamond measured by scanning probe methods

Y Iseri[1], M Honda[2,6], Y-D Kim[3], T Ando[4], W Choi[5] and H Tomokage[2]

[1] Kyushu Mitsumi Co., Ltd, 1049 Tateiwa, Iizukai, Fukuoka 820-8533, Japan
[2] Department of Electronics Engineering and Computer Science, Fukuoka University, 8-19-1 Nanakuma, Jonan-ku, Fukuoka 814-0180, Japan
[3] Department of Material Science and Engineering, Busan University, 30 Changjeon-dong, Keumjeong-ku, Busan 609-735, Korea
[4] Fukuoka Industry, Science and Technology Foundation, 1-1-1 Tenjin, Chuo-ku, Fukuoka 810-0001, Japan
[5] National Institute for Materials Science, 1-1 Namiki, Tsukuba, Ibaragi 305-0047, Japan

Received 31 July 2003
Published 22 December 2003
Online at stacks.iop.org/JPhysCM/16/S171 (DOI: 10.1088/0953-8984/16/2/020)

Abstract

Scanning tunnelling microscopy (STM) and current imaging tunnelling current spectroscopy (CITS) methods were performed on polycrystalline diamond films grown on silicon substrates grown by microwave plasma-enhanced chemical vapour deposition. Large tunnelling currents were observed at some grain boundaries and crystal surfaces with secondary grains. Following atomic force microscopy (AFM) measurements, we performed scanning probe contact current (SPCC) measurements to investigate the spatial variation of electrical resistance on the surface by using an AFM cantilever in contact mode. The conducting grain boundaries and facets were observed on both boron-doped and undoped samples. For microscale characterization of the field emission properties, we performed scanning probe field emission current (SPFEC) measurements. From the results of STM/CITS, AFM/SPCC and SPFEC, it is concluded that the specific grain boundaries and facets on polycrystalline diamonds work as initial points of electron emission and cause high field emission current through a conducting pass formed in the bulk.

(Some figures in this article are in colour only in the electronic version)

1. Introduction

Chemically vapour deposited (CVD) diamond has been intensively studied for applications to the field emission cathode because of its stable high electron emission at low electric field [1–6].

[6] Current address: Fujitsu, 4-1-1 Kamikodanaka, Nakahara-ku, Kawasaki, Kanagawa 211-8588, Japan.

© 2004 IOP Publishing Ltd Printed in the UK

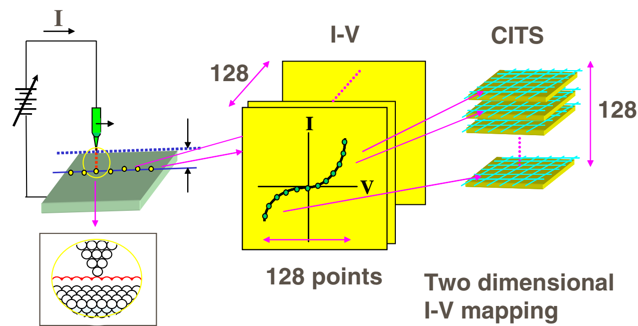

Figure 1. Schematic diagram of STM and CITS measurements. The local I–V characteristics were measured at 128 × 128 pixel points in a vacuum of 2×10^{-8} Pa.

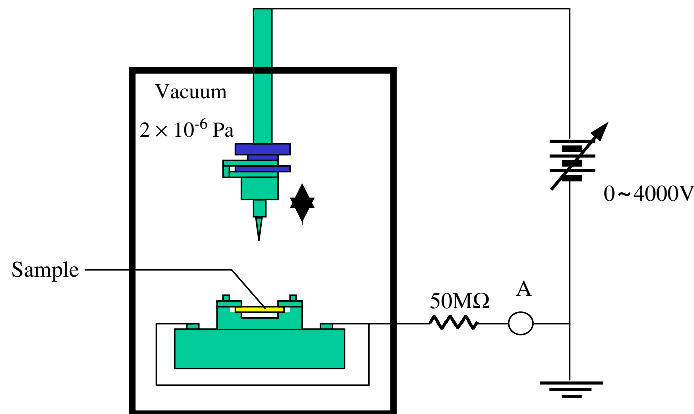

Figure 2. Schematic diagram of the SPFEC measurement apparatus.

Diamond has a negative electron affinity after the termination of hydrogen on (111) surfaces, which is a strong advantage for field emission display (FED) applications [7]. Also CVD diamond has a highly conductive p-type layer on the surface after hydrogen plasma treatment in a CVD chamber [8].

Field emission properties depend on surface morphology and electrical conductivity as well as the electron surface state. It is known that field emission on diamond film occurs randomly under a parallel electrode which is positively biased to derive electrons from the surface. We performed scanning tunnelling microscopy (STM) on boron-doped polycrystalline diamond and found that the electron emission initiated at some grain boundaries of the secondary grains grown on specific crystalline facets [9]. Zhang *et al* [10], on the other hand, performed local resistance measurements using a cantilever of atomic force microscopy (AFM) as the contact probe. They found conducting channels on diamond films grown by the hot-filament CVD method. However, they did not compare their result to field emission measurements. A more comprehensive understanding of the electron emission mechanism at both the nanoscale and microscale is needed to determine the potential of developing a highly efficient cold cathode for FED applications.

In this study, we applied three scanning probe methods of STM [11], AFM and scanning probe field emission current (SPFEC) measurement [12] to boron-doped and undoped diamonds in order to clarify the relation between the conducting layer and electron emission

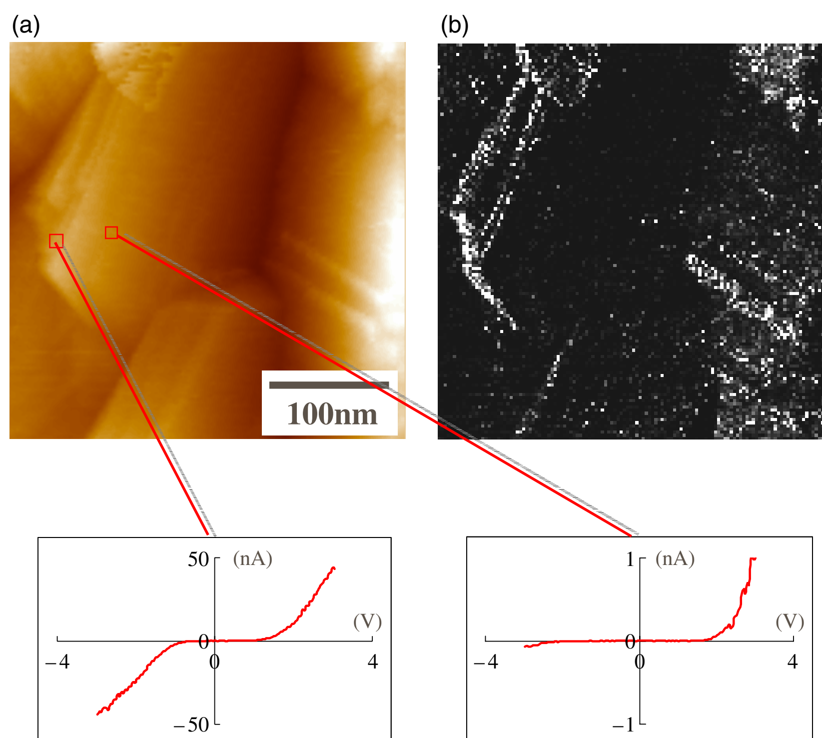

Figure 3. (a) STM and (b) CITS images on boron-doped polycrystalline diamond grown for 6 h with growth conditions of 1% methane and 0.77 ppm B_2H_6. The I–V characteristics were obtained at high and low emission points.

properties. STM and current imaging tunnelling spectroscopy (CITS) were employed for nanoscale characterization [9]. We also performed AFM and scanning probe contact current (SPCC) measurements. SPCC uses an AFM cantilever as a contact probe, and measures a spatial variation of surface resistance in contact mode under a fixed voltage. As for microscale field emission characterization, we performed SPFEC measurements to obtain the mapping of the emission current. Electron emission sites at both nanoscale and microscale were investigated for various doping conditions and deposition times. From the results of the STM/CITS, AFM/SPCC and SPFEC, it is concluded that the grain boundaries on specific facets work as initial emission sites and cause the high field emission current through a conducting pass formed in the bulk.

2. Experimental procedure

The microwave plasma enhanced CVD method was employed to grow boron-doped and undoped diamond films on p- and n-type silicon substrates. Methane and hydrogen were used as the main reactant gases, and B_2H_6 gas was used as a doping source. The methane concentration was varied from 0.6% to 3.0% while keeping the total gas pressure at 50 Torr. For boron-doped samples, the B_2H_6 concentration was 0.77 or 2.0 ppm. Before deposition, the silicon substrates were polished using diamond abrasives and subsequently cleaned with acetone, methanol and distilled water for 10 min respectively in an ultrasonic bath. Silicon

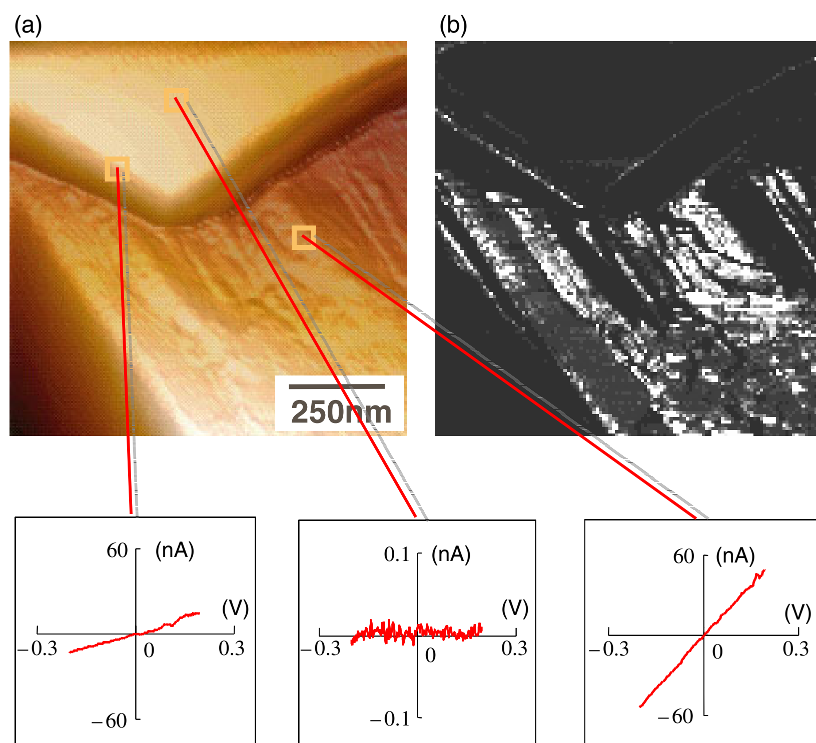

Figure 4. (a) AFM and (b) SPCC images on undoped diamond grown for 6 h with a growth condition of 1% methane. The local I–V characteristics were obtained at three different points in figure 4(a).

substrates were also cleaned in hydrogen plasma for 5 min in the CVD chamber. A microwave source of 2.45 GHz and 800 W was used, and the substrate surface temperature was controlled at about 750 °C by using an automatic substrate cooling system and was monitored by a disappearing-filament pyrometer. Diamond films were deposited for 3, 6 and 12 h and all samples were hydrogen terminated for 10 min under the same conditions after deposition.

The film quality was checked using field emission scanning electron microscopy (FE/SEM) and confocal Raman spectroscopy. Ultra-high vacuum scanning tunnelling microscopy (STM, JEOL JSM 4610) was used to evaluate the structure and quality of the films. Figure 1 shows the schematic diagram of the CITS measurement. The local I–V characteristic was measured at each pixel point in a vacuum of 2×10^{-8} Pa and the CITS image under a fixed voltage was displayed as well as the STM image. The I–V characteristics were measured at 128×128 pixel points. The approach currents were 0.2–0.5 nA and 0.05–0.1 nA for boron-doped and undoped samples, respectively.

In order to obtain the spatial variation of electrical resistance on the surface, we performed SPCC measurements using a JSM-4210 (JEOL) with a silicon cantilever coated by platinum to reduce the probe resistance. The local I–V characteristic was also obtained by varying the bias voltage.

Figure 2 shows the schematic diagram of the SPFEC measurement apparatus: the sample was set in a vacuum of about 5×10^{-5} Pa. A tungsten tip was used as a probe. A positive voltage up to 4000 V was applied to the tip with respect to sample surface. By keeping the

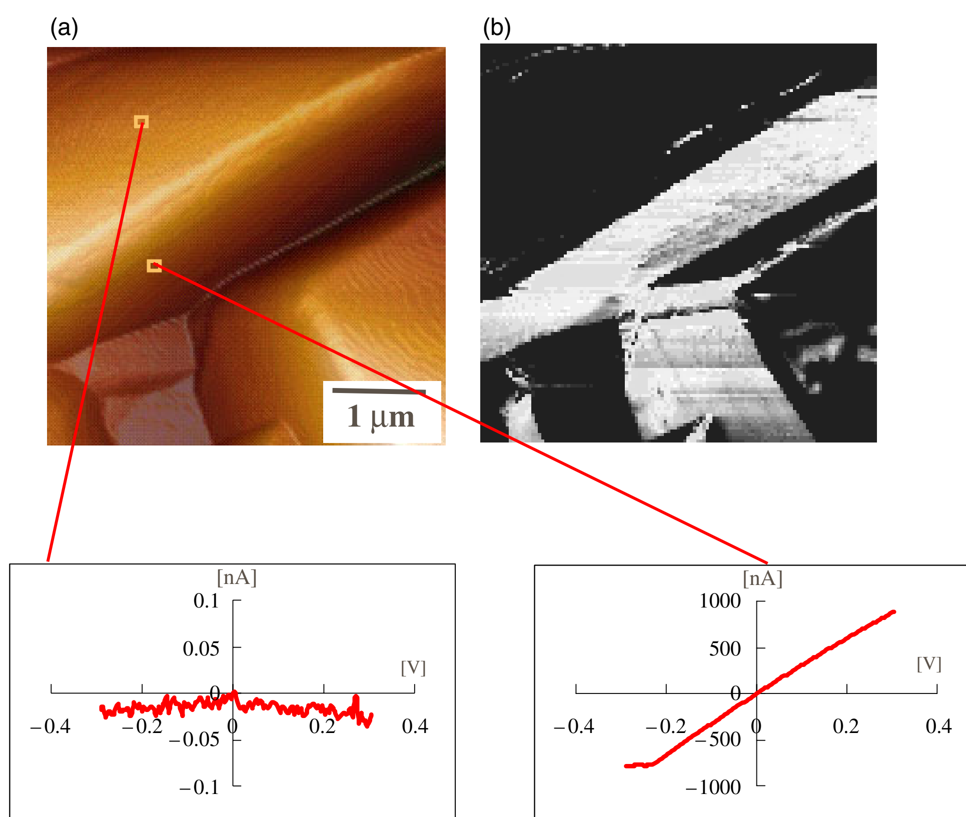

Figure 5. (a) AFM and (b) SPCC images on undoped diamond. The growth condition was the same as in figure 4.

distance between the surface and the tip constant, the computer-controlled stage was moved by 1 mm × 1 mm in the x and y directions, and the field emission current mapping was obtained at a microscale.

3. Results and discussion

From SEM observations, we found well-developed randomly oriented crystalline planes. The surface roughness increased with deposition time and secondary grains on a crystalline facet were observed in the sample deposited for 12 h. All the samples showed a sharp Raman peak around 1333 ± 1 cm^{-1}. There was no particular difference in surface morphology between p- and n-type silicon substrates.

Figure 3 shows STM and CITS images of size 330 nm × 330 nm obtained for boron-doped diamond films grown for 6 h with growth conditions of 1% methane and 0.77 ppm B_2H_6. The white region in figure 3(b) indicates the high current area. It can be seen that some grain boundaries on specific facets emit electrons, which do not necessarily correspond to the peak positions morphologically. These results are in agreement with the results of Frolov *et al* [13] using scanning tunnelling field emission microscopy (STFEM). The local I–V characteristics at high and low electron emission positions are also shown in figure 3. Both results show the non-linear behaviour typical for a tunnelling current, although there is a difference in current of

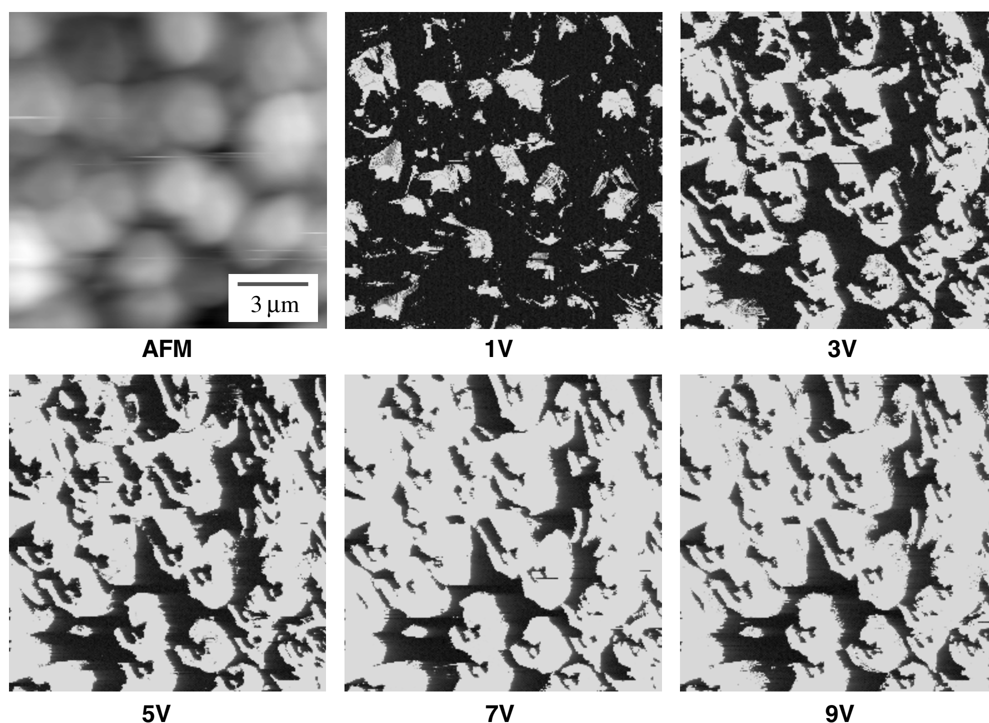

Figure 6. SPCC images for various bias voltages on undoped diamond grown for 6 h with 1% methane.

more than one order of magnitude between the high and low emission positions. It was difficult to obtain an STM image for the undoped sample, because of the high resistivity in diamond film. However, we could obtain STM images in rare cases even on undoped samples. It should be explained that some of the grain boundary was electrically conductive and was connected to the surface conductive layer formed by hydrogen termination. In the high magnification case of size 20 nm $\times$ 20 nm, it was found that some grain boundaries emitted electrons at first, and the white area expanded to almost the whole area on increasing the bias voltage. This indicates that electron emission initiates at some grain boundaries on specific crystalline facets.

Figure 4 shows AFM and SPCC images obtained for undoped diamond grown for 6 h with 1% CH_4. The white area in figure 4(b) indicates the high current region. It can be seen that a crystalline facet and some boundaries between facets are conductive, although no doping gas was introduced in the CVD chamber. It can be seen that the local I–V characteristics at two points in figure 4(a) show Ohmic behaviour. However, the current in another facet is less than 0.01 nA at ± 0.3 V, indicating an insulating surface. Figure 5 is another result of AFM and SPCC obtained for undoped diamond. The growth condition was the same as in figure 4. It is noted that some grain boundaries and some crystalline facets near grain boundaries are conductive. It was found that the resistance in some facets was very low even for the undoped case. A similar result was obtained for the boron-doped case. The conductive grain boundaries for undoped diamonds should be formed by the incorporation of impurity atoms. It was considered that impurity atoms such as residual atoms in the CVD chamber precipitated along the grain boundary. It is known that CVD (111) diamonds treated in hydrogen plasma after deposition have a p-type conducting layer due to hydrogen termination. We considered that

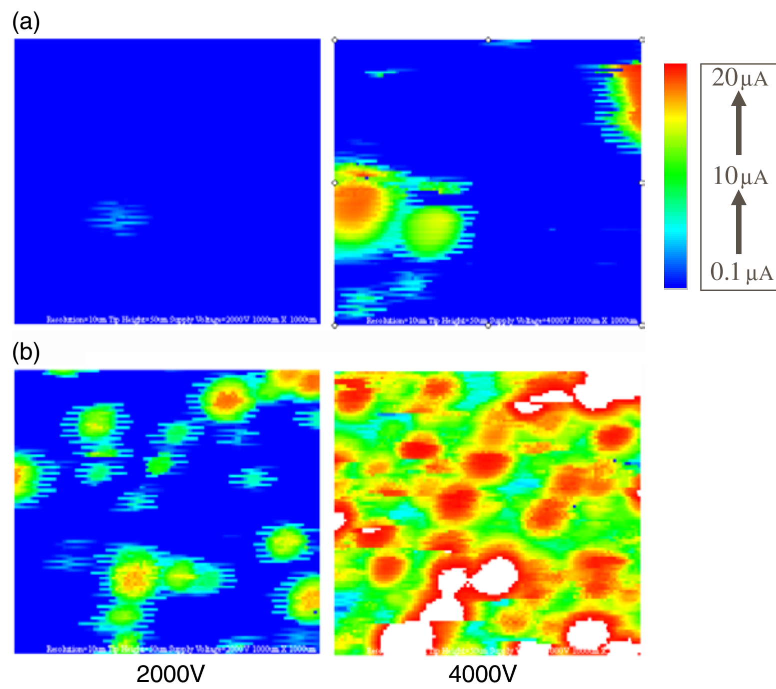

Figure 7. SPFEC images for (a) undoped diamond and (b) boron-doped diamond grown for 6 h with 2 ppm B_2H_6.

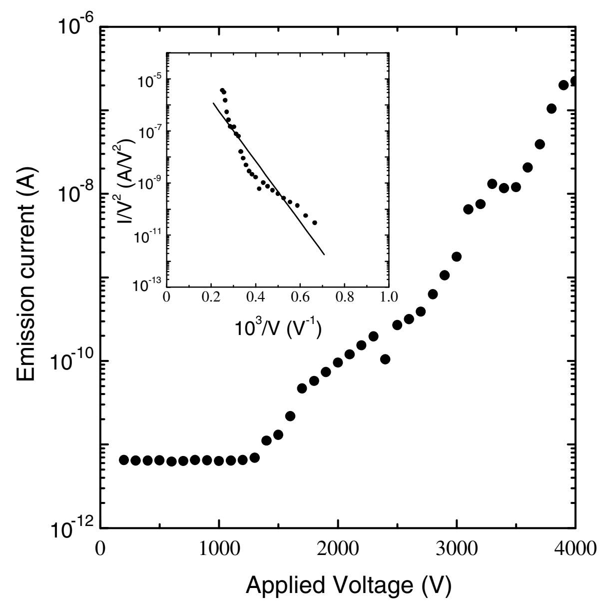

Figure 8. The local I–V characteristic in the high emission region of figure 7. The inset is the Fowler–Nordheim plot.

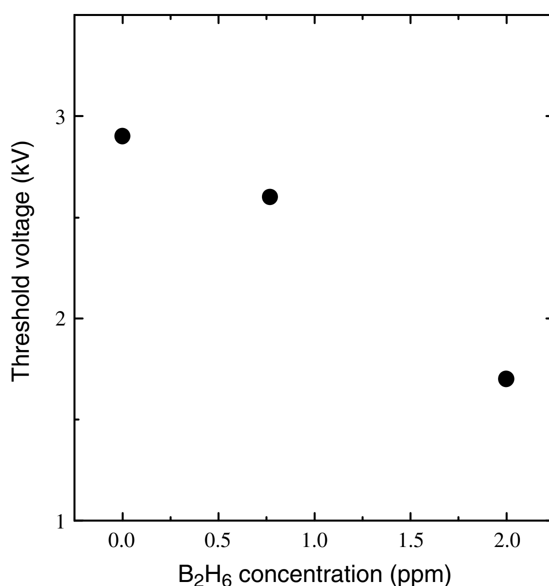

Figure 9. The threshold voltage versus boron doping concentration.

once the conductive grain boundaries were formed, the surface layer became conductive to the boundary, resulting in low resistance areas in the SPCC image. Figure 6 is the result of SPCC measurement on undoped diamond grown for 6 h with 1% methane for various bias voltages. It can be seen in figure 6 that the white area spreads on increasing the bias voltage. There are some regions where the current remains very low even under the bias condition of 7 V. Therefore it is considered that the resistivity in bulk diamond is high although the conducting grain boundary is formed because of the incorporation of impurity atoms.

Figure 7 is the result of SPFEC measurements for undoped diamond and boron-doped diamond with 2 ppm B_2H_6. The spacing between surface and tip was 30 μm, and 2000 and 4000 V were applied to the tip by changing the position over an area of 1 mm $\times$ 1 mm. It can be seen that random emission sites also exist at a microscale. Figure 8 is the I–V plot in the high emission region of figure 7(a), where the inset is a Fowler–Nordheim plot indicating the field emission current characteristic. It has been reported that for diamond and diamond-like carbon, the activation process under high electric field causes a stable increase in field emission current [12]. The current was measured at least five times, and the stabilized I–V characteristic was plotted in figure 8. We define here the threshold voltage which causes 1 nA current from the I–V plot. Figure 9 shows the threshold voltage for various boron concentrations. It can be seen that the threshold voltage decreases with doping concentration. This should be due to lowering the resistance in diamond by adding boron atoms. On the other hand, the threshold voltage for undoped diamond was higher than that for boron-doped diamond, and had the lowest value in the case of 3 h. The increase in threshold voltage with deposition time for the undoped case might be explained by the increase in the electrically isolated area on diamond.

As a result, the following mechanism is deduced for electron emission from polycrystalline diamond. The grain boundaries on specific facets work as initial emission sites. In the high current region, the p-type conducting surface and conductive grain boundaries make the current pass from the electrode to the emission site. Therefore both the surface state and the grain boundary are keys to fabricate a diamond cathode with high efficiency.

4. Summary

We performed STM/CITS, AFM/SPCC and SPFEC measurements on boron-doped and undoped polycrystalline diamond films. From nanoscale characterization, a high current was observed at some grain boundaries. This indicates that electron emission initiates at some grain boundaries on specific crystalline facets. The surface resistance was low at some boundaries and facets even for undosed diamond, which suggests that the current flows to the surface mainly through the conducting pass which shows Ohmic behaviour. An increase in boron-doping concentration caused a decrease in threshold voltage, whereas for undoped diamond the threshold voltage increased with deposition time. This suggests that the conducting pass is important for field emission as well as the surface state on crystalline facets.

Acknowledgments

The authors would like to thank Mr T Sato, Mr K Sueyoshi and Ms Y Takashima of JEOL for helping with the AFM and SPCC measurements. This work was supported by CREATE, Japan.

References

[1] Muto Y, Sugino T and Shirafuji J 1991 *Appl. Phys. Lett.* **59** 843
[2] Hong D and Aslam M 1995 *J. Vac. Sci. Technol.* B **13** 427
[3] Lamouri A, Wang Y, Mearini G T, Krainsky I L, Dayton J A Jr and Mueller W 1996 *J. Vac. Sci. Technol.* B **14** 2046
[4] Geis M W, Efremow N N, Krohn K E, Twichell J C, Lyszczar T M, Kalish R, Greer J A and Tabat M D 1998 *Nature* **393** 431
[5] Proffitt S S, Probert S J, Whitfield M D, Foord J S and Jackman R B 1999 *Diamond Relat. Mater.* **8** 768
[6] Nishimura M, Ogawa K, Hatta A and Ito T 1999 *Diamond Relat. Mater.* **7** 754
[7] Liu J, Zhirnov V V, Myers A F, Wojak G J, Choi W B, Hren J J, Wolter S D, McClure M T, Stoner B R and Glass J T 1995 *J. Vac. Sci. Technol.* B **13** 422
[8] Grot S A, Gildenblat G Sh, Hatfield C W, Wronski C R, Badzian A R, Badzian T and Messier R 1990 *IEEE Electron Device Lett.* **11** 100
[9] Kim Y-D, Choi W, Wakimoto H, Usami S, Tomokage H and Ando T 1999 *Appl. Phys. Lett.* **75** 3219
[10] Zhang L, Sakai T, Sakuma N, Ono T and Nakayama K 1999 *Appl. Phys. Lett.* **75** 3527
[11] Cannaerts M, Nesladek M, Remes Z, Van Haesendonck C and Stals L M 2000 *Phys. Status Solidi* a **181** 77
[12] Kim Y-D, Choi W, Wang C-H, Ando T, Jeon H, Chang S-Y and Tomokage H 2002 *Japan. J. Appl. Phys.* **41** 3081
[13] Frolov V D, Karabutov A V, Konov V I, Pimenov S M and Prokhorov A M 1999 *J. Phys. D: Appl. Phys.* **32** 815